ACS OMEGA

http://pubs.acs.org/journal/acsodf

Article

Analysis of Operation Conditions of $Ca(OH)_2$ Entrained Carbonator Reactors for CO_2 Capture in Backup Power Plants

Yolanda Alvarez Criado* and Borja Arias

Cite This: *ACS Omega* 2022, 7, 28093−28100

Read Online

ACCESS | Metrics & More | Article Recommendations

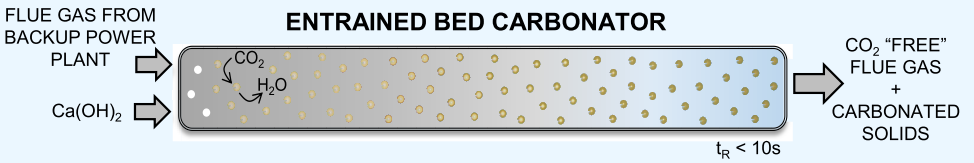

ABSTRACT: The share of renewables in the energy sector is increasing, and energy storage and backup power combustion systems to cover the periods of time with low renewable energy production are becoming increasingly needed. Flexible calcium looping configurations based on the storage of solids are a promising alternative to capture the CO_2 produced in such backup combustion systems. The use of $Ca(OH)_2$ instead of CaO is better suited to these applications due to the faster reaction kinetics and higher carbonation conversions as $Ca(OH)_2$ in powder form can achieve conversions of up to 0.7 in just a few seconds at temperatures of 550−650 °C. To take advantage of these fast reaction kinetics, compact carbonator reactors with short gas−solid contact times (i.e., a few seconds) can be designed. However, the low enthalpy of the carbonation reaction of $Ca(OH)_2$ makes it challenging to find the optimum conditions which maximize the CO_2 capture efficiency. In this work, a basic entrained reactor with recent experimental reaction kinetics has been used to determine suitable operational windows for this kind of carbonator. CO_2 capture efficiencies above 90% can be achieved for flue gases with low CO_2 concentrations ($4\%_v$ CO_2) when they are fed into the carbonator at temperatures of around 500−600 °C while maintaining low F_{Ca}/F_{CO2} ratios (<2) and feeding the sorbent at ambient temperature. When capturing from a flue gas with a higher CO_2 concentration ($14\%_v$ CO_2), the sorbent needs to be fed at higher temperatures to effectively capture CO_2 in short contact times (i.e., 6 s).

1. INTRODUCTION

Drastic changes in the energy sector are required to achieve full decarbonatization by 2050 and limit the global temperature increase.[1−3] These future energy scenarios rely on the use of renewable energy (such as wind, solar, and so forth) with shares above 80%.[4] There is a wide consensus that backup power systems will be needed in these scenarios to cover periods without enough power supply from renewables. For this purpose, combustion power plants coupled with CO_2 capture can be used to complement renewable energy storage systems.[5]

The capture of the intermittently produced CO_2 in such combustion backup power plants operating at very low capacity factors (i.e., 0.1−0.2)[6,7] presents technical and economic challenges.[8−10] Calcium looping (CaL) systems have been demonstrated to be highly flexible by storing the Ca-sorbent in low-cost reservoirs, which allows decoupling the capture of CO_2 from the sorbent regeneration.[11−15] The use of $Ca(OH)_2$ instead of CaO as a sorbent can increase the potential of CaL due to the higher reaction kinetics and maximum carbonation conversions that the sorbent can achieve and maintain along cycling.[16−19] Experimental studies have shown that Ca/CO_2 molar ratios close to 1.3 would be sufficient to remove 90% of CO_2;[18] meanwhile, molar ratios of 5−10 are typically required when using CaO.[20,21] This would drastically reduce the amount of sorbent fed into the carbonator as well as the size of the solid handling and storage systems.

$Ca(OH)_2$ produced by hydration of CaO presents poor fluidization properties, making the use of circulating fluidized bed carbonators challenging. Entrained bed gas−solid reactor configurations are better suited to handle this kind of particle. Indeed, these types of reactors have been proposed for CO_2 capture using fine CaO particles as a sorbent in cement plants[21−23] and energy storage applications.[24] Other reactor configurations such as multiple cyclonic reactors connected in a tower to achieve a countercurrent gas−solid contact, similar to pre-calciners of cement and lime industries, could also be used.[25] For post-combustion CO_2 capture using CaO as a sorbent, long entrained bed reactors with several tens of meters are needed to ensure sufficient gas−solid contact times

Received: April 6, 2022
Accepted: July 21, 2022
Published: August 4, 2022

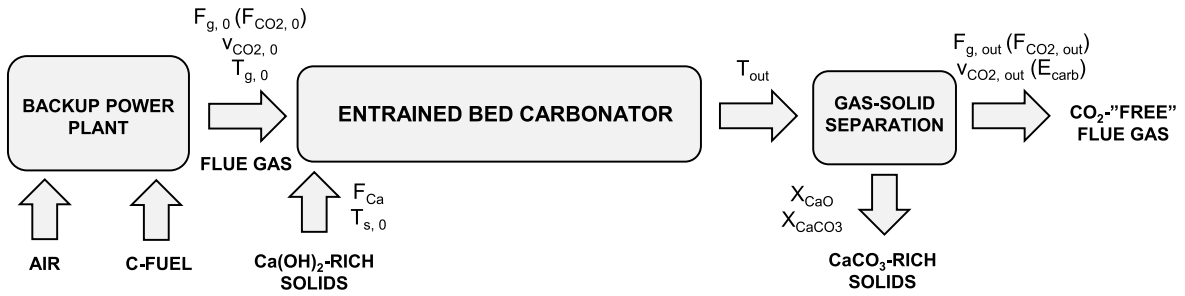

Figure 1. Schematic representation of the $Ca(OH)_2$ entrained bed carbonator for the CO_2 capture from flue gases produced in a backup fossil fuel power plant.

(typically around 20 s) and sorbent conversion. However, $Ca(OH)_2$ particles can achieve carbonation conversions of around 0.7 at temperatures of 550−650 °C and CO_2 concentrations in the range of 5−25%$_v$ in less than 6 s of gas−solid contact times,[19] therefore facilitating the design of more compact reactors.

Another important aspect is the low carbonation enthalpy of $Ca(OH)_2$ when compared to that of CaO (72 vs 176 kJ/mol at 650 °C). This could facilitate the control of the temperature in the entrained carbonator reactor avoiding the need of a costly energy recovery system from the carbonation reaction. However, the low reaction enthalpy is a challenge to the operation of the carbonator at suitable temperatures even if it is operated in close-to-adiabatic conditions.[26] Moreover, the need for storing the sorbent at temperatures below 400 °C to avoid $Ca(OH)_2$ dehydration[27] would hinder the operation at high carbonation temperatures.

The objective of this work is to identify suitable operation windows for entrained bed carbonator reactors. A basic reactor model has been developed by including the $Ca(OH)_2$ reaction kinetics obtained in recent experimental work.[19] A sensitivity analysis of the main variables affecting the CO_2 capture efficiency has been carried out. These variables include the conditions of the flue gas (temperature and CO_2 concentration) and the temperature and flow of the sorbent at the inlet of the reactor.

2. CARBONATOR REACTOR MODEL AND REACTION KINETICS

A basic steady-state 1D reactor model has been developed for the entrained bed carbonator shown in Figure 1. In this model, the conditions were considered to only change in the axial direction, with the radial dispersion being negligible. A plug flow is assumed for both the gas and solid phases. Due to the low $Ca(OH)_2$ particle size considered (<5 μm), it has been assumed that the slip velocity between the gas and the solids is negligible. In addition, due to the operation with a low diluted suspension, the particle and wall-particle interactions were ignored. The gas phase is assumed to follow the ideal gas equation, and the $Ca(OH)_2$ solids are assumed to be of a constant average particle size. As an approximation, it has been assumed that the reactor operates at adiabatic conditions, and only heat transfer between the gas and solid phases is taken into account. Heat losses in the reactor would lead to a decrease in the carbonation temperature and conversions achieved.

To solve the mass and energy balances (as shown schematically in Figure 2), the reactor was divided into 20 elements as the model results were independent of a higher

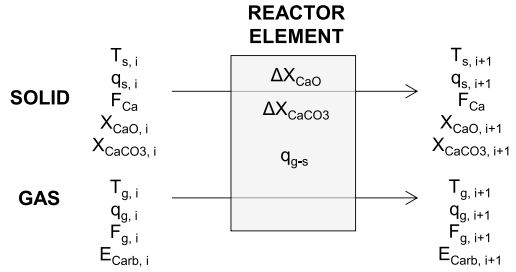

Figure 2. Schematic representation of the main parameters used for the mass and heat balances in a reactor element and their nomenclature.

number of elements. For simplicity, the gas−solid residence time (t_R) has been chosen as a characteristic design parameter.

The molar flows (F in mol/s) at each reaction element were calculated from mass balances (eqs 1−6), by taking into account the solids dehydration (X_{CaO}) and carbonation (X_{CaCO3}) conversions, as described below.

$$F_{g,i} = F_{inert} + F_{CO2,i} + F_{H2O,i} \quad (1)$$

$$F_{CO2,i+1} = F_{CO2,i} - X_{CaCO3,i} F_{Ca} \quad (2)$$

$$F_{H2O,i+1} = F_{H2O,i} + X_{CaO,i} F_{Ca} \quad (3)$$

$$F_{Ca} = F_{Ca(OH)2,i} + F_{CaO,i} + F_{CaCO3,i} \quad (4)$$

$$F_{CaO,i} = X_{CaO,i} F_{Ca} \quad (5)$$

$$F_{CaCO3,i} = X_{CaCO3,i} F_{Ca} \quad (6)$$

The CO_2 capture efficiency (E_{Carb}) is calculated as

$$E_{Carb,i} = 1 - \frac{F_{CO2,i}}{F_{CO2,0}} \quad (7)$$

The heat balances to the gas and solid streams have been calculated according to eqs 8 and 9 to assess the temperature at each element i, considering an adiabatic reactor ($q_s = q_g = 0$).

$$q_{g,i+1} = F_{g,i+1}C_{pg,i+1}(T_{g,i+1} + 273) - F_{g,i}C_{pg,i}(T_{g,i} + 273) + q_{g-s,i+1} \quad (8)$$

$$q_{s,i+1} = F_{s,i+1}C_{ps,i+1}(T_{s,i+1} + 273) - F_{s,i}C_{ps,i}(T_{s,i} + 273) - q_{g-s,i+1} + \Delta H_{CaO}(X_{CaO,i+1} - X_{CaO,i})F_{Ca} - \Delta H_{CaCO3}(X_{CaCO3,i+1} - X_{CaCO3,i})F_{Ca} \quad (9)$$

https://doi.org/10.1021/acsomega.2c02134
ACS Omega 2022, 7, 28093−28100

Table 1. Properties of the Gas and Solids Obtained from Data Available in the Literature[a,28,29]

compound	molar density, ρ (mol/m^3)	specific heat, C_p (kJ/mol K)	thermal conductivity, k (W/mK)
CO_2	calculated according to the ideal gas equation	$4.3\cdot10^{-2} + 1.2\cdot10^{-5}\,T - 817.2/T^2$	$4.3\cdot10^{-8}\,T^2 + 4.2\cdot10^{-5}\,T$
H_2O		$3.4\cdot10^{-2} + 6.3\cdot10^{-7}\,T + 5.6\cdot10^{-9}\,T^2$	$5.3\cdot10^{-8}\,T^2 + 4.5\cdot10^{-5}\,T$
N_2		$2.7\cdot10^{-2} + 4.2\cdot10^{-6}\,T$	$-4.3\cdot10^{-8}\,T^2 + 9.9\cdot10^{-5}\,T$
O_2		$3.5\cdot10^{-2} + 1.1\cdot10^{-6}\,T - 784.6/T^2$	$-2.8\cdot10^{-8}\,T^2 + 9.7\cdot10^{-5}\,T$
$Ca(OH)_2$	29.9×10^3	$9.0\cdot10^{-2} + 2.9\cdot10^{-5}\,T$	
$CaCO_3$	27.1×10^3	$10.0\cdot10^{-2} + 2.7\cdot10^{-5}\,T - 2152.3/T^2$	
CaO	59.6×10^3	$5.0\cdot10^{-2} + 4.5\cdot10^{-6}\,T - 693.9/T^2$	

[a]Please notice that in this table T = temperature in K.

where C_p is the specific heat obtained from equations available in the literature[28] and summarized in Table 1 and ΔH_{CaO} and ΔH_{CaCO3} are the reaction heats of the endothermic $Ca(OH)_2$ dehydration (104 kJ/mol) and the exothermic CaO carbonation (176 kJ/mol), respectively. The heat transfer rate between the gas and solid phases (q_{g-s}) is calculated according to eq 10:

$$q_{g-s,i+1} = a_{g-s,i+1} h_{g-s,i+1} (T_{g,i+1} - T_{s,i+1}) \quad (10)$$

with a_{g-s} and h_{g-s} being the contact surface and the convective heat transfer coefficient between the gas and particles, respectively,[28] as given in eqs 11 and 12.

$$a_{g-s,i+1} = \frac{6}{d_p} Q_{s,i+1} t_{R,i} \quad (11)$$

$$h_{g-s,i+1} = \frac{k_{g,i+1} Nu_{g-s,i+1}}{d_p} \quad (12)$$

where Q_s is the volumetric flow of the solid phase, d_p is the particle size of the solids, k_g is the thermal conductivity of the gas as a function of the temperature obtained from data available in the literature[29] and summarized in Table 1, and Nu_{g-s} is the dimensionless Nusselt number. For the calculation of the Nusselt number, several correlations in literature can be found, mainly depending on the gas and solid velocities.[28]

For simplicity, the Nu_{g-s} in eq 12 has been taken as a constant value along the reactor. To illustrate the effect of this parameter, the model has been solved for an extreme case with inlet gas and solid temperatures of 600 and 20 °C, respectively, and assuming different values of Nu_{g-s}. The results obtained are shown in Figure 3. As can be seen, the temperatures of both phases converge after 0.4 s of contact time even for very low Nusselt numbers. For $Nu_{g-s} > 0.1$, there are no significant differences in the temperature profiles. Therefore, a conservative Nu_{g-s} of 0.1, typical for pneumatic conveying systems,[30] has been used to estimate the convective heat transfer coefficient between the gas and particles.

The sorbent conversion has been calculated as a function of the gas−solid residence time in each reactor element. Based on the data available in the literature,[31−34] it can be assumed that the reaction proceeds through an initial decomposition of $Ca(OH)_2$, followed by the carbonation of the formed nascent CaO under the conditions expected in the entrained carbonator (i.e., fine powders, short reaction times, and so forth). In recent experimental work,[19] a particle model was proposed for the $Ca(OH)_2$ carbonation for temperatures between 350 and 650 °C assuming an almost instantaneous carbonation of the nascent CaO under the conditions expected in the entrained carbonator. This work also showed that the carbonation of $Ca(OH)_2$ can be considered independent of the

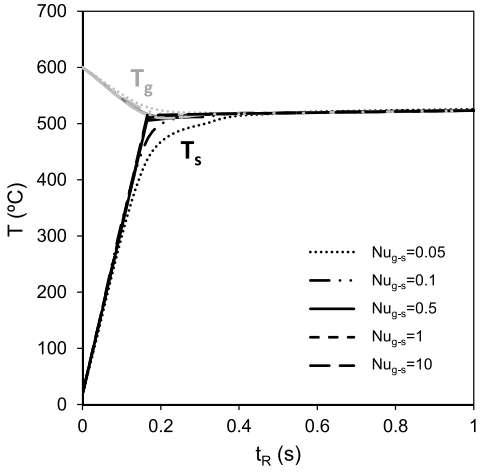

Figure 3. Evaluation of the effect of the Nusselt number (Nu_{g-s}) over the evolution of the gas and solid temperatures (T_g and T_s) with the gas−solid residence time (t_R) for a reference case, where $T_{g,0}$ = 600 °C and $T_{s,0}$ = 20 °C.

CO_2 concentration for molar fractions ($\nu_{CO2} = F_{CO2}/F_g$) up to 0.25. The results obtained in this work revealed that the presence of water vapor on the reacting atmosphere has less influence on the sorbent carbonation conditions expected in the entrained carbonator treating flue gases with maximum concentrations of 15%$_v$ H_2O. This result could be explained due to the modest equilibrium H_2O partial pressure (about 8%$_v$ H_2O for a temperature of 400 °C using eq 13 from Barin[35]).

$$P_{eq,H2O} = 2.30 \times 10^8 \exp\left(-\frac{11607}{T + 273}\right) \quad (13)$$

According to eq 14, the dehydration conversion is estimated using a simplified shirking core model with chemical reaction control,[27]

$$X_{CaO,i} = 1 - \left(1 - A_{Dehy} \exp\left(-\frac{E_{a,Dehy}}{R(T_{s,i} + 273)}\right) t_{R,i}/3\right)^3 \quad (14)$$

where $t_{R,i}$ is the residence time in each element, $T_{s,i}$ is the temperature of the solids, A_{Dehy} is the pre-exponential factor, and $E_{a,Dehy}$ is the activation energy. A_{Dehy} and $E_{a,Dehy}$ take values of 4359 s^{-1} and 63.2 kJ/mol, respectively.[19] Then, the carbonation conversion is calculated assuming that the nascent CaO reacts with the CO_2 present in the gas phase up to its maximum conversion (X_{Max}) of 0.7:[19]

$$X_{CaCO3,i} = 0.7 \cdot X_{CaO,i} \quad (15)$$

https://doi.org/10.1021/acsomega.2c02134
ACS Omega 2022, 7, 28093−28100

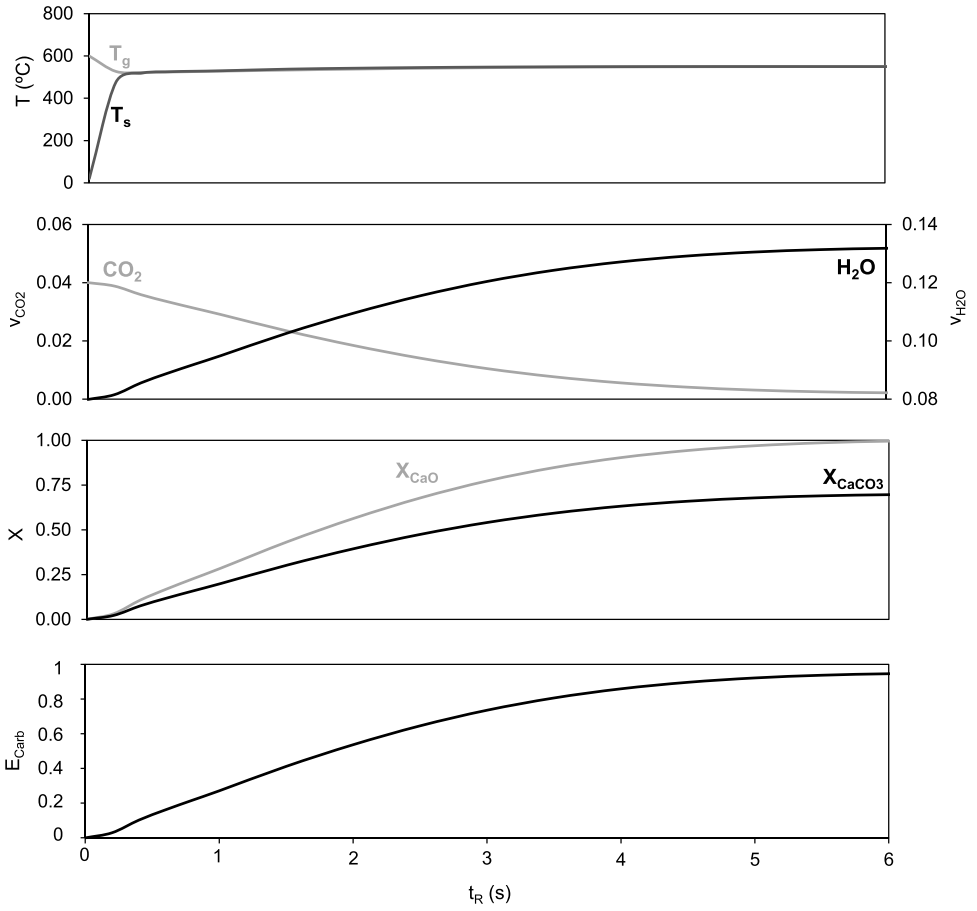

Figure 4. Evolution of the temperatures of the gas and solids (T_g and T_s), CO_2 and H_2O molar fractions (ν_{CO2} and ν_{H2O}), solids conversion to CaO and $CaCO_3$ (X_{CaO} and X_{CaCO3}), and CO_2 capture efficiency (E_{Carb}) with the gas−solid residence time (t_R). Reference case for $\nu_{CO2,0}$ = 0.04, $\nu_{H2O,0}$ = 0.08, $T_{g,0}$ = 600 °C, $T_{s,0}$ = 20 °C, and F_{Ca}/F_{CO2} = 1.36.

According to this assumption, the overall reaction enthalpy (ΔH_{global}, in kJ per mol of CaO) can be calculated as follows:

$$\Delta H_{global} = X_{CaO}(0.7 \cdot \Delta H_{CaCO3} - \Delta H_{CaO}) \quad (16)$$

3. RESULTS AND DISCUSSION

To identify feasible operation windows, five main operation variables have been analyzed: the gas−solid residence time in the carbonator, the CO_2 inlet concentration, the inlet temperatures of the gases and solids, and the Ca/CO_2 molar ratio. For the entrained bed reactor configuration, a gas−solid residence time t_R < 10 s has been taken in all cases. Two different flue gas compositions have been considered, which are representative of two different combustion backup power plants. One corresponds to the flue gas produced in a gas turbine with a typical CO_2 concentration of 4%$_v$. The other corresponds to a conventional power plant using biomass or coal as the fuel with a 14%$_v$ CO_2. In both cases, a total flue gas molar flow of 10 kmol/s has been considered. Different integration arrangements for the carbonator reactor within the flue gas path of the backup power plant could be proposed. In the first case, the flue gas can be fed directly into the carbonator after the gas turbine, with typical outlet temperatures of 500−650 °C. If it is part of a combined cycle, it could also be fed after the heat recovery steam generator (HRSG) with temperatures around 120 °C.[36] In the case of the conventional power plant, there could be different integration schemes by treating the flue gas directly after the combustion chamber or at different points of the heat recovery system.[17,18] To assess these integration scenarios, the effect of a wide range of inlet gas temperatures of up to 850 °C on the carbonator performance has been studied. The effect of the temperature of the inlet solids has been analyzed in order to explore the possibility of storing solids at ambient temperature or the need of a preheating step of the sorbent before being fed into the reactor. On the other hand, the dehydration of the $Ca(OH)_2$ has to be minimized during storage. Thus, inlet temperatures ranging from 20 °C to up to a maximum of 400 °C have been assessed.

Figure 4 illustrates the evolution of the temperatures of the gas and solids, the CO_2 and H_2O molar fractions, the conversion of the solid to CaO and $CaCO_3$, and the CO_2 capture efficiency as a function of the gas−solid residence time for a natural gas turbine case with a flue gas consisting of 4%$_v$ CO_2, 8%$_v$ H_2O, 12%$_v$ O_2, and 76%$_v$ N_2 and a carbonator gas inlet temperature of 600 °C. In this example, the $Ca(OH)_2$ sorbent is injected at ambient temperature. A molar ratio F_{Ca}/F_{CO2} of 1.36 has been chosen, which is the minimum ratio needed to achieve an E_{carb} = 0.95 assuming a maximum sorbent conversion of 0.7. As can be seen in this figure, the maximum capture efficiency of 0.95 is achieved for a gas−solid residence time of 6 s.

An average temperature of 543 °C for the streams of gas and solids is reached at the exit of the reactor. This temperature is lower than the inlet flue gas temperature, showing that the

https://doi.org/10.1021/acsomega.2c02134
ACS Omega 2022, 7, 28093−28100

overall carbonation heat (19 kJ/mol, according to eq 16) is not enough to compensate for the sensible heat required to heat up the solids entering the bed. Thus, the heat balance in the carbonator is governed by the inlet temperatures of the flue gas and the solids due to the low reaction enthalpy. In the case of the gas turbine backup power plant, the temperature of the flue gas plays a major role due to the low requirement of the sorbent associated with the reduced CO_2 concentration in the flue gas. The effect of this variable can be seen in Figure 5,

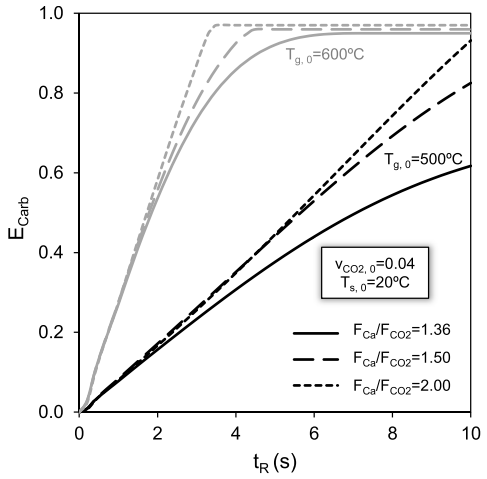

Figure 5. CO_2 capture efficiency (E_{Carb}) as a function of the gas−solid residence time (t_R) for different flue gas temperatures ($T_{g,0}$ = 500 °C in black and $T_{g,0}$ = 600 °C in gray) and F_{Ca}/F_{CO2} ratios ($\nu_{CO2,0}$ = 0.04, $T_{s,0}$ = 20 °C).

where E_{carb} is represented as a function of the gas−solid residence time for two flue gas inlet temperatures. If the flue gas is fed into the carbonator at a temperature of 600 °C, a CO_2 capture efficiency above 0.95 can be achieved for a gas−solid residence time of 6 s. However, the E_{carb} is largely reduced when the inlet gas temperature is 500 °C. In this case, a maximum E_{Carb} value of only 0.60 can be reached for a gas−solid residence time of 10 s. Under these conditions, the CO_2 capture efficiency can be increased by using a higher F_{Ca}/F_{CO2} molar ratio. Thus, an E_{Carb} of 0.93 can be achieved when F_{Ca}/F_{CO2} = 2 for a gas−solid residence time of 10 s. This molar ratio has a moderate impact for reaction times above 6 s when the flue gas is fed into the carbonator at 600 °C as the fast carbonation kinetics ensure the maximum sorbent carbonation (up to 0.7). However, increasing the F_{Ca}/F_{CO2} ratio to 2 allows CO_2 capture efficiencies above 0.90 to be reached in even shorter reaction times (i.e., in less than 3 s) when the gas is fed at 600 °C.

The effect of the sorbent inlet temperature on the CO_2 capture efficiency is shown in Figure 6. The results presented have been calculated for an F_{Ca}/F_{CO2} ratio of 1.36 and a gas−solid residence time in the reactor of 6 s. This figure also shows the temperature at the carbonator outlet (left axis). As can be seen, there is a maximum drop of the temperature between the gas inlet and the outlet of around 50−60 °C when the sorbent is fed at ambient temperature, which can be moderated by feeding the sorbent at higher temperatures. Regarding the CO_2 capture efficiency, gas temperatures above 570 °C are necessary to reach E_{Carb} > 0.9 when $T_{s,0}$ = 20 °C. This gas inlet temperature could be reduced down to 510 °C if the solids enter the reactor at 400 °C. It is interesting to note that,

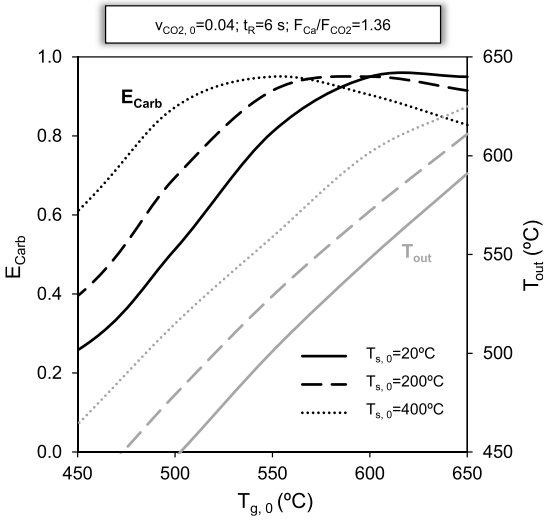

Figure 6. Effect of the gas inlet temperature ($T_{g,0}$) on the CO_2 capture efficiency (E_{Carb} in black) and the carbonator outlet temperature (T_{out} in gray) for different solids inlet temperatures ($T_{s,0}$) being $\nu_{CO2,0}$ = 0.04, t_R = 6 s, and F_{Ca}/F_{CO2} = 1.36.

when feeding solids at temperatures above 200 °C, E_{Carb} decreases if $T_{g,0}$ > 550 °C (see Figure 6). In this case, the temperature reached at the exit of the carbonator limits the minimum CO_2 concentration that can be achieved given by the equilibrium.

Based on the above discussion, gas entering the carbonator at temperatures of between 500 and 650 °C would be required to achieve high capture efficiencies for typical flue gases of gas turbines with a 4%$_v$ CO_2. These temperatures are within the range of those found at the exit of commercial turbines allowing the flue gas to be fed directly into the carbonator.[37] If these turbines are part of a combined cycle power plant, the flue gas cannot be fed into the carbonator at the exit of the HRSG due to its low temperature (i.e., around 120 °C). In this case, the carbonator should be integrated between the exit of the turbine and the HRSG. However, temperature drops of up to 60 °C in the gas entering the HRSG may be expected, which could negatively affect the global energy efficiency.

Regarding the case of a biomass/coal power plant, a flue gas with a 14 and 8%$_v$ of CO_2 and H_2O, respectively, has been considered. Figure 7 shows an example of the effect of the F_{Ca}/F_{CO2} ratio on the CO_2 capture efficiency. For this example, an inlet flue gas temperature of 650 °C has been chosen. In this case, the effect of the inlet solid temperature is more relevant due to the larger sorbent requirements in the carbonator associated with the greater CO_2 concentration. If the solids are fed at ambient temperature, the increase of the F_{Ca}/F_{CO2} ratio has a negative effect on the CO_2 capture efficiency. This is a result of the decrease in the average temperature in the carbonator, which reduces the sorbent conversion. However, there is a clear improvement when introducing the solids in the carbonator at higher temperatures, with an E_{Carb} of 0.95 being reached in 5 s if solids are fed at 200 °C. Under these conditions, the carbonation efficiency can be improved to 0.99 by increasing the F_{Ca}/F_{CO2} ratio to a value of 2.

The effect of the flue gas inlet temperature on the CO_2 capture efficiency and the temperature at the exit of the carbonator can be seen in Figure 8. When the solids are fed at ambient temperature, the temperature drop between the flue gas at the inlet and outlet can be as high as 200 °C. As a result,

https://doi.org/10.1021/acsomega.2c02134
ACS Omega 2022, 7, 28093−28100

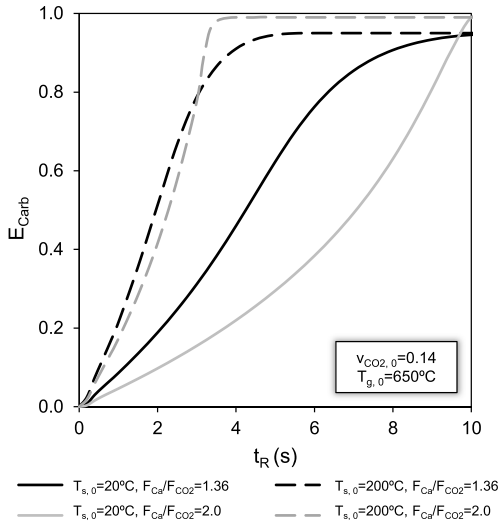

Figure 7. CO_2 capture efficiency (E_{Carb}) as a function of the gas−solid residence time for a flue gas with $\nu_{CO2,0}$ = 0.14 at $T_{g,0}$ = 650 °C, F_{Ca}/F_{CO2} ratios of 1.36 (in black) and 2.0 (in gray), and solids input temperatures ($T_{s,0}$) of 20 °C (full line) and 200 °C (dashed line).

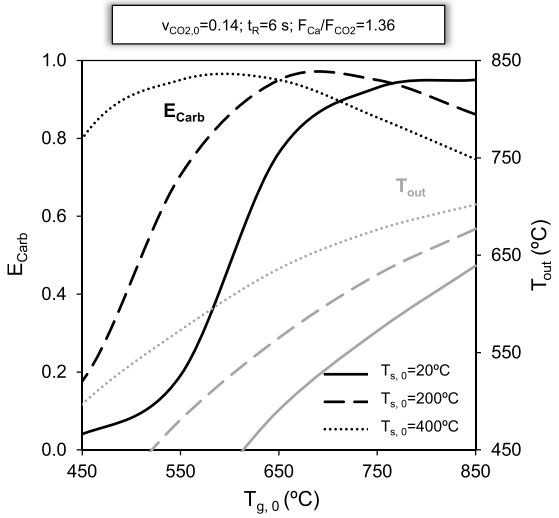

Figure 8. Effect of the gas ($T_{g,0}$) and solids inlet temperatures ($T_{s,0}$) on the CO_2 capture efficiency (E_{Carb} in black) and the carbonator outlet temperature (T_{out} in gray) being $\nu_{CO2,0}$ = 0.14, t_R = 6 s, and F_{Ca}/F_{CO2} = 1.36.

$T_{g,0}$ > 700 °C are needed to achieve a CO_2 capture efficiency of 0.9. These temperatures can only be reduced by feeding the sorbent at higher temperatures. Thus, $T_{g,0}$ of around 500 and 600 °C would be sufficient if the inlet temperatures of the sorbent are 400 and 200 °C, respectively, as shown in Figure 8.

Based on the above results, in a conventional biomass/coal power plant, the strategy to integrate the carbonator should be the extraction of the flue gas in the convective section, in a similar arrangement to that proposed by Phalak et al.,[17] where flue gas temperatures above 650 °C can be found. In this case, the storing or preheating of the sorbent at temperatures above 200 °C would increase the CO_2 capture efficiency and help moderate the required flue gas inlet temperature.

4. CONCLUSIONS

In this work, feasible operation windows to capture CO_2 using $Ca(OH)_2$ as the sorbent in an adiabatic entrained bed carbonator have been analyzed. For this purpose, a basic reactor model with the experimentally obtained reaction kinetics has been developed. Mass and heat balances have been solved in order to evaluate the effect of different variables, such as the inlet temperatures of the gas (between 450 and 850 °C) and solids (between 20 and 400 °C), the gas−solid residence times, the CO_2 concentration in the gas (for cases with 4 and 14%$_v$), and the Ca/CO_2 molar ratio (between 1.36 and 2) on the carbonator performance.

The results of this analysis indicate that the flue gas needs to enter the carbonator reactor at high temperatures due to the low reaction enthalpy of the $Ca(OH)_2$ carbonation. Thus, temperatures above 550 °C are required to ensure CO_2 capture efficiencies of above 0.9 in less than 6 s when the flue gas has a 4%$_v$ CO_2 and the sorbent is fed at 20 °C. In the case of flue gases with 14%$_v$ CO_2, the sorbent needs to be fed into the carbonator at temperatures above 200 °C to maintain an inlet gas temperature at around 600 °C. Low F_{Ca}/F_{CO2} ratios (below 2) can ensure capture efficiencies above 0.90 when $Ca(OH)_2$ is used as the CO_2 sorbent. Therefore, high CO_2 capture efficiencies can be reached with very short reaction times if gas and solid temperatures are optimized. The results presented in this work highlight the potential of using powdery $Ca(OH)_2$ as the sorbent to ensure fast kinetics and high sorbent carbonation conversions.

AUTHOR INFORMATION

Corresponding Author

Yolanda Alvarez Criado − *Consejo Superior de Investigaciones Científicas, CSIC-INCAR, 33011 Oviedo, Spain;* orcid.org/0000-0003-2962-7061; Phone: +34 985119090; Email: yolanda.ac@incar.csic.es; Fax: +34 985297662

Author

Borja Arias − *Consejo Superior de Investigaciones Científicas, CSIC-INCAR, 33011 Oviedo, Spain;* orcid.org/0000-0001-9613-5388

Complete contact information is available at: https://pubs.acs.org/10.1021/acsomega.2c02134

Notes

The authors declare no competing financial interest.

ACKNOWLEDGMENTS

The authors acknowledge the financial support provided by the European Union under the Research Fund for Coal and Steel (RFCS) Program (BackCap Project, GA 10103400) and by the Spanish Ministry of Science and Innovation under the R&D Program Oriented to Challenges of the Society (RTI2018-097224-B-I00). Support from Prof. J.C. Abanades García during the preparation of this manuscript is also acknowledged.

NOMENCLATURE

a	surface area between gas and particles, m^2
A_{Dehy}	pre-exponential factor for the dehydration reaction, s^{-1}
C_p	specific heat, kJ/mol K
d_p	particle size, m

https://doi.org/10.1021/acsomega.2c02134
ACS Omega 2022, 7, 28093−28100

E_{Carb}	CO_2 capture efficiency
$E_{a,Dehy}$	activation energy of the dehydration reaction, kJ/mol
F	molar flow, mol/s
h	convective heat transfer coefficient, W/m^{2}K
k	thermal conductivity, W/mK
Nu	Nusselt dimensionless number
P	pressure, kPa
q	heat transfer rate, W
Q	volumetric flow, m^3/s
R	gas constant, kJ/mol K
T	temperature, °C
t_R	gas−solid residence time, s
X	Ca molar conversion
ΔH	reaction enthalpy, kJ/mol
ΔX	conversion increment
ν	molar fraction, calculated as F_i/F_g
ρ	molar density, mol/m^3

Subscripts

0	at the inlet of the bed
Ca	active Ca material
$CaCO_3$	Ca to $CaCO_3$
CaO	Ca to CaO
CO_2	carbon dioxide
eq	equilibrium
g	gas phase
global	global including the dehydration and carbonation reactions
g−s	gas−solid transfer
H_2O	water vapor
inert	inert gases
out	at the outlet of the bed
s	solid phase

REFERENCES

(1) IPCC. *Global Warming of 1.5°C. An IPCC special report on the impacts of global warming of 1.5°C above pre-industrial levels and related global greenhouse gas emission pathways, in the context of strengthening the global response to the threat of climate change*; Cambridge University Press: Cambridge, UK, 2018.

(2) IEA. *European Union 2020: Energy policy review*; Internaltional Energy Agency: Paris, France, 2020.

(3) UNFCCC. Glasgow climate pact - Proposal by the President; *United Nations Framework Convention on Climate Change*,2021.

(4) Tsiropoulos, I.; Nijs, W.; Tarvydas, D.; Ruiz Castello, P. *Towards net-zero emissions in the EU energy system by 2050 − Insights from scenarios in line with the 2030 and 2050 ambitions of the European Green Deal, EUR 29981 EN*; Luxembourg, 2020.

(5) IRENA. *Innovation landscape for a renewable-powdered future: Solutions to integrate variable renewables*; International Renewable Energy Agency, 2019.

(6) Brouwer, A. S.; van den Broek, M.; Seebregts, A.; Faaij, A. Operational flexibility and economics of power plants in future low-carbon power systems. *Appl. Energy* **2015**, *156*, 107−128.

(7) Abdilahi, A. M.; Mustafa, M. W.; Abujarad, S. Y.; Mustapha, M. Harnessing flexibility potential of flexible carbon capture power plants for future low carbon power systems: review. *Renew. Sustain. Energy Rev.* **2018**, *81*, 3101−3110.

(8) Craig, M. T.; Zhai, H.; Jaramillo, P.; Klima, K. Trade-offs in cost and emission reductions between flexible and normal carbon capture and sequestration under carbon dioxide emission constraints. *Int. J. Greenh. Gas Control* **2017**, *66*, 25−34.

(9) Abanades, J. C.; Arias, B.; Lyngfelt, A.; Mattisson, T.; Wiley, D. E.; Li, H.; Ho, M. T.; Mangano, E.; Brandani, S. Emerging CO_2 capture systems. *Int. J. Greenh. Gas Control* **2015**, *40*, 126−166.

(10) Bui, M.; Adjiman, C. S.; Bardow, A.; Anthony, E. J.; Boston, A.; Brown, S.; Fennell, P. S.; Fuss, S.; Galindo, A.; Hackett, L. A.; Hallett, J. P.; Herzog, H. J.; Jackson, G.; Kemper, J.; Krevor, S.; Maitland, G. C.; Matuszewski, M.; Metcalfe, I. S.; Petit, C.; Puxty, G.; Reimer, J.; Reiner, D. M.; Rubin, E. S.; Scott, S. A.; Shah, N.; Smit, B.; Trusler, J. P. M.; Webley, P.; Wilcox, J.; Mac Dowell, N. Carbon Capture and Storage (CCS): The way forward. *Energy Environ. Sci.* **2018**, *11*, 1062−1176.

(11) Criado, Y. A.; Arias, B.; Abanades, J. C. Calcium Looping CO_2 capture system for back-up power plants. *Energy Environ. Sci.* **2017**, *10*, 1994−2004.

(12) Astolfi, M.; De Lena, E.; Romano, M. C. Improved flexibility and economics of Calcium Looping power plants by thermochemical energy storage. *Int. J. Greenh. Gas Control* **2019**, *83*, 140−155.

(13) Astolfi, M.; De Lena, E.; Casella, F.; Romano, M. C. Calcium Looping for power generation with CO_2 capture: The potential of sorbent storage for improved economic performance and flexibility. *Appl. Therm. Eng.* **2021**, *194*, No. 117048.

(14) Arias, B.; Criado, Y. A.; Abanades, J. C. Thermal integration of a flexible Calcium Looping CO_2 capture system in an existing back-up coal power plant. *ACS Omega* **2020**, *5*, 4844−4852.

(15) Abanades, J. C.; Arias, B.; Criado, Y. A. System and method for energy storage using circulating fluidized bed combustors. EP2762781, 2013.

(16) Yu, F.-C.; Phalak, N.; Sun, Z.; Fan, L.-S. Activation strategies for calcium-based sorbents for CO_2 capture: A perspective. *Ind. Eng. Chem. Res.* **2011**, *51*, 2133−2142.

(17) Phalak, N.; Wang, W.; Fan, L.-S. $Ca(OH)_2$-based Calcium Looping process development at The Ohio State University. *Chem. Eng. Technol.* **2013**, *36*, 1451−1459.

(18) Fan, L. S.; Ramkumar, S.; Wang, W.; Statnick, R. Carbonation calcination reaction process for CO_2 capture using a highly regenerable sorbent. US8512661B2, 2013.

(19) Arias, B.; Criado, Y. A.; Pañeda, B.; Abanades, J. C. Carbonation kinetics of $Ca(OH)_2$ under Conditions of entrained reactors to capture CO_2. *Ind. Eng. Chem. Res.* **2022**, *61*, 3272−3277.

(20) Charitos, A.; Rodríguez, N.; Hawthorne, C.; Alonso, M.; Zieba, M.; Arias, B.; Kopanakis, G.; Scheffknecht, G.; Abanades, J. C. Experimental validation of the Calcium Looping CO_2 capture process with two circulating fluidized bed carbonator reactors. *Ind. Eng. Chem. Res.* **2011**, *50*, 9685−9695.

(21) Plou, J.; Martínez, I.; Grasa, G. S.; Murillo, R. Experimental carbonation of CaO in an entrained flow reactor. *React. Chem. Eng.* **2019**, *4*, 899−908.

(22) Spinelli, M.; Martínez, I.; Romano, M. C. One-dimensional model of entrained-flow carbonator for CO_2 capture in cement kilns by Calcium Looping process. *Chem. Eng. Sci.* **2018**, *191*, 100−114.

(23) Turrado, S.; Arias, B.; Fernández, J. R.; Abanades, J. C. Carbonation of fine CaO particles in a drop tube reactor. *Ind. Eng. Chem. Res.* **2018**, *57*, 13372−13380.

(24) Karasavvas, E.; Scaltsoyiannes, A.; Antzaras, A.; Fotiadis, K.; Panopoulos, K.; Lemonidou, A.; Voutetakis, S.; Papadopoulou, S. One-dimensional heterogeneous reaction model of a drop-tube carbonator reactor for thermochemical energy storage applications. *Energies* **2020**, *13*, 5905.

(25) Chen, W.-C.; Ouyang, S.; Huang, C.-H.; Shen, C.-H.; Hsu, H.-W. Loop tower CO_2 capture system, carbonator, calciner and operating method thereof. US9610537B2, 2017.

(26) Wang, W.; Ramkumar, S.; Wong, D.; Fan, L. S. Simulations and process analysis of the carbonation−calcination reaction process with intermediate hydration. *Fuel* **2012**, *92*, 94−106.

(27) Criado, Y. A.; Alonso, M.; Abanades, J. C. Kinetics of the CaO/$Ca(OH)_2$ hydration/dehydration reaction for thermochemical energy storage applications. *Ind. Eng. Chem. Res.* **2014**, *53*, 12594−12601.

(28) Perry, R. B.; Green, D. W. *Perry's chemical engineers' handbook*; McGraw-Hill, 1999.

(29) Huber, M.; Harvey, A. *Thermal conductivity of gases*; CRC-Press: Boca Raton, FL, 2011.

https://doi.org/10.1021/acsomega.2c02134
ACS Omega 2022, 7, 28093−28100

(30) Rajan, K. S.; Dhasandhan, K.; Srivastava, S. N.; Pitchumani, B. Studies on gas−solid heat transfer during pneumatic conveying. *Int. J. Heat Mass Transfer* **2008**, *51*, 2801−2813.
(31) Blamey, J.; Lu, D. Y.; Fennell, P. S.; Anthony, E. J. Reactivation of CaO-based sorbents for CO_2 capture: Mechanism for the carbonation of $Ca(OH)_2$. *Ind. Eng. Chem. Res.* **2011**, *50* (17), 10329−10334.
(32) Materic, V.; Smedley, S. I. High temperature carbonation of $Ca(OH)_2$. *Ind. Eng. Chem. Res.* **2011**, *50*, 5927−5932.
(33) Montes-Hernandez, G.; Chiriac, R.; Toche, F.; Renard, F. Gas−solid carbonation of $Ca(OH)_2$ and CaO particles under non-isothermal and isothermal conditions by using a thermogravimetric analyzer: Implications for CO_2 capture. *Int. J. Greenh. Gas Control* **2012**, *11*, 172−180.
(34) Yu, J.; Zeng, X.; Zhang, G.; Zhang, J.; Wang, Y.; Xu, G. Kinetics and mechanism of direct reaction between CO_2 and $Ca(OH)_2$ in micro fluidized bed. *Environ. Sci. Technol.* **2013**, *47*, 7514−7520.
(35) Barin, I. *Thermochemical Data of Pure Substances*; VCH Verlagsgesellschaft: Weinheim, Germany, 1989.
(36) DOE/NETL. *Cost and performance baseline for fossil energy plants volume 1a: Bituminous coal (PC) and natural gas to electricity. Revision 3*; US Department of Energy, National Energy Technology Laboratory, 2015.
(37) Siemens. Reliable gas turbines https://www.siemens-energy.com/global/en/offerings/power-generation/gas-turbines.html.

https://doi.org/10.1021/acsomega.2c02134
ACS Omega 2022, 7, 28093−28100